

Anomalous Metallic State in the Vicinity of Metal to Valence-Bond Solid Insulator Transition in LiVS_2

N. Katayama,^{1,*} M. Uchida,² D. Hashizume,² S. Niitaka,² J. Matsuno,² D. Matsumura,³ Y. Nishihata,³ J. Mizuki,³ N. Takeshita,⁴ A. Gauzzi,^{1,5} M. Nohara,^{1,†} and H. Takagi^{1,2,4}

¹Department of Advanced Materials, University of Tokyo, Kashiwa 277-8561, Japan

²RIKEN (The Institute of Physical and Chemical Research), Wako 351-0198, Japan

³Synchrotron Radiation Research Center, Japan Atomic Energy Agency, Hyogo 679-5148, Japan

⁴Correlated Electron Research Center (CERC), National Institute of Advanced Industrial Science and Technology (AIST), Tsukuba 305-8562, Japan

⁵Institut de Minéralogie et de Physique des Milieux Condensés, Université Pierre et Marie Curie-Paris 6 and CNRS, 4, place Jussieu, 75252, Paris, France

(Received 16 April 2009; published 2 October 2009)

We investigate LiVS_2 and LiVSe_2 with a triangular lattice as itinerant analogues of LiVO_2 known for the formation of a valence-bond solid (VBS) state out of an $S = 1$ frustrated magnet. LiVS_2 , which is located at the border between a metal and a correlated insulator, shows a first order transition from a paramagnetic metal to a VBS insulator at $T_c \sim 305$ K upon cooling. The presence of a VBS state in the close vicinity of insulator-metal transition may suggest the importance of itinerancy in the formation of a VBS state. We argue that the high temperature metallic phase of LiVS_2 has a pseudogap, likely originating from the VBS fluctuation. LiVSe_2 was found to be a paramagnetic metal down to 2 K.

DOI: 10.1103/PhysRevLett.103.146405

PACS numbers: 71.30.+h, 61.50.Ks, 61.66.-f

Transition metal compounds with a geometrically frustrated lattice, such as a triangular or a pyrochlore lattice, often form a valence-bond solid (VBS) state at low temperatures. When the t_{2g} orbitals are partially occupied, utilizing orbital degrees of freedom, complex “molecular” clusters in a spin-singlet state are often formed: trimer in LiVO_2 [1–5], heptamer in AlV_2O_4 [6], helical dimer in MgTi_2O_4 [7], and octamer in CuIr_2S_4 [8]. A VBS state was also found in organic systems with geometrical frustration [9]. Very recently, Shimizu *et al.* demonstrated that the VBS state can be melted by applying hydrostatic pressure P on the organic compound $\text{EtMe}_3\text{P}[\text{Pd}(\text{dmit})_2]_2$ with a triangular lattice. Remarkably, superconductivity appears as soon as the VBS state is suppressed by P [10].

A question that arises is whether or not similar melting of the VBS state and appearance of exotic metallic phases can occur in inorganic frustrated systems. In the inorganic systems, however, the application of external pressure is expected not to melt but to stabilize VBS due to a predominant volume effect. In CuIr_2S_4 , the lattice shrinks appreciably in the VBS perhaps due to the formation of strongly bonded singlet molecules, and the VBS can be stabilized through the $-pV$ (p , pressure; V , volume) term in the corresponding free energy [11,12]. The effects of negative pressure on the VBS states of inorganic systems, on the other hand, have not been investigated so far.

The inorganic LiVO_2 in which the magnetic V^{3+} ions ($3d^2$, $S = 1$) form a triangular lattice is known to be a paramagnetic insulator with strong antiferromagnetic interactions between the localized $S = 1$ moments at high temperatures. Upon cooling, at $T_c \sim 500$ K, LiVO_2 exhib-

its a first order phase transition to a VBS state with a characteristic spin gap of ~ 1600 K, evidenced by the formation of vanadium trimers. With this system, one can apply “negative” pressure by replacing oxygen with larger anions such as S and Se [13–16]. Moreover, the negative pressure may increase the overlap between the V $3d$ and p orbitals (O: $2p$, S: $3p$, and Se: $4p$) and also increase the electronic bandwidth. Thus, this vanadium-based triangular system provides a good opportunity to study the effects of negative pressure on VBS states in inorganic materials.

In this Letter, we demonstrate that LiVS_2 is indeed an itinerant analogue of LiVO_2 with suppressed VBS, as shown in Fig. 1. We found that in LiVS_2 , a phase transition from a paramagnetic metal to a trimer VBS insulator occurs at $T_c \sim 305$ K, which is lower than that of LiVO_2 . In LiVSe_2 with highest negative pressure, the phase transition is suppressed down to 2 K. In the high temperature metallic phase of LiVS_2 , strong temperature dependence of the bulk susceptibility, χ , was observed, which is similar to the pseudogap behavior found in underdoped superconducting cuprates. We argue that this is evidence for a pseudogap formation by short-range spin-singlet fluctuations in the paramagnetic metallic phase of LiVS_2 .

Powder samples of LiVS_2 , LiVSe_2 , and their solid solution $\text{LiVS}_{2-x}\text{Se}_x$ were prepared by a soft-chemical method followed by a solid-state reaction. For $\text{LiVS}_{2-x}\text{Se}_x$ ($0 \leq x \leq 0.4$), Li-deficient $\text{Li}_{\sim 0.75}\text{VS}_{2-x}\text{Se}_x$ was obtained first by a reaction of an appropriate amount of Li_2S , V, S, and Se in an evacuated quartz tube at 700°C for 3 days. For LiVSe_2 , VSe_2 was synthesized from an appropriate

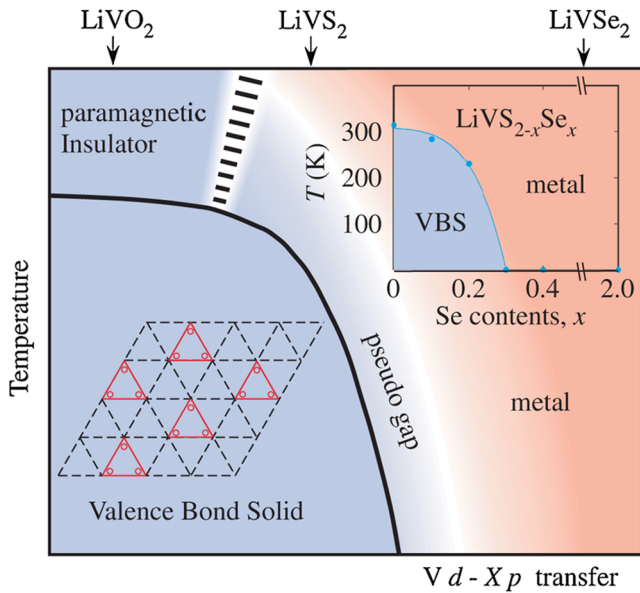


FIG. 1 (color online). Schematic phase diagram in the LiVO_2 , LiVS_2 , and LiVSe_2 system. Spin pseudogap is observed in the white region in the metallic phase. The left inset shows the schematic VBS state on the triangular lattice of V^{3+} . The circles within the triangles denote the V ions. The right inset shows the phase diagram in the vicinity of the VBS transition. Solid circles denote the VBS transition obtained from magnetic measurements for the solid solution $\text{LiVS}_{2-x}\text{Se}_x$.

amount of V and Se at the same condition with $\text{Li}_{\sim 0.75}\text{VS}_{2-x}\text{Se}_x$. The products were immersed in a 0.2 M *n*-BuLi hexane solution for 4 days to attain the maximum Li content [14]. The samples were characterized by powder x-ray diffraction. The electron diffraction measurements were carried out in a HF-3000S (Hitachi) transmission electron microscope. Differential scanning calorimetry (DSC) was conducted by using DSC 204 F1 Phoenix (Netzsch). Vanadium *K*-edge extended x-ray absorption fine structure (EXAFS) was measured at BL14B1, SPring-8. Magnetic susceptibility was measured by a SQUID magnetometer (Quantum Design). Electrical resistivity was measured by a four-probe method. The powder samples were sintered at 500 °C under Ar atmosphere for the resistivity measurements.

LiVS_2 exhibits a first order metal to insulator transition at $T_c \sim 305$ K, shown in Fig. 2. At high temperatures above T_c , the resistivity is about 40 m Ω cm and almost temperature independent. Since the sample is a low-temperature sintered polycrystal, empirically, the intrinsic resistivity can be more than 1 order of magnitude smaller than 40 m Ω cm, consistent with the metallic nature. Accompanied with the metal to insulator transition, an abrupt decrease in the magnetic susceptibility is observed, as shown in Fig. 2. The system is very likely to be non-magnetic below T_c with a temperature-independent Van Vleck term and a tiny low-temperature Curie tail, which

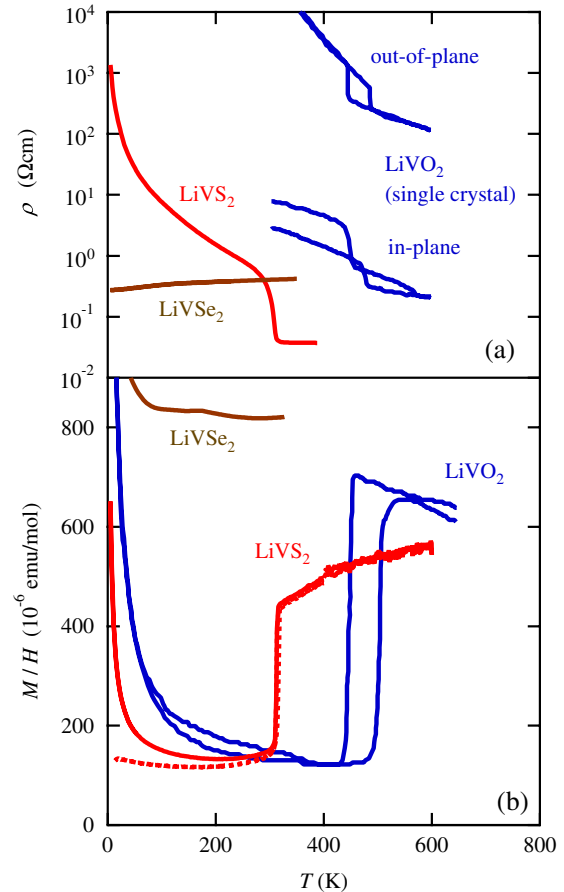


FIG. 2 (color online). (a) Electrical resistivity and (b) magnetic susceptibility of LiVO_2 , LiVS_2 , and LiVSe_2 as a function of temperature. The electrical resistivity and magnetic susceptibility data of LiVO_2 are cited from Ref. [5]. The broken line in magnetic susceptibility has been corrected for paramagnetic impurities as explained in the text.

corresponds to paramagnetic impurities of $\sim 1\%$ if we assume spin-1/2 moment. In accord with the nonmagnetic behavior of LiVS_2 , ^{51}V NMR relaxation rate T_1^{-1} shows thermally activated behavior, from which we estimate a spin gap of $\Delta = 1900$ K [17].

Despite the metallic behaviors above T_c , electron diffraction measurements on LiVS_2 show an evidence for the formation of the V trimers below T_c , which indicates development of the same VBS state as in the insulating LiVO_2 . The electron diffraction pattern reveals sharp superlattice reflections at $\{1/3\ 1/3\ 0\}$ below $T_c \sim 305$ K, as in Fig. 3. The superlattice reflections correspond to a $\sqrt{3}a \times \sqrt{3}a$ superlattice in real space, suggesting a formation of vanadium trimers in the VS_2 plane, shown in the right inset of Fig. 3. The Fourier-transformed patterns of EXAFS spectra, shown in Fig. 3, are indeed consistent with the vanadium trimers in low-temperature phase. Below T_c , spectra show three clear peaks between 1.5 and 3.5 Å. The first peak at around 2 Å is ascribed to that from the first-neighbored V-S. The second and third peaks, marked by

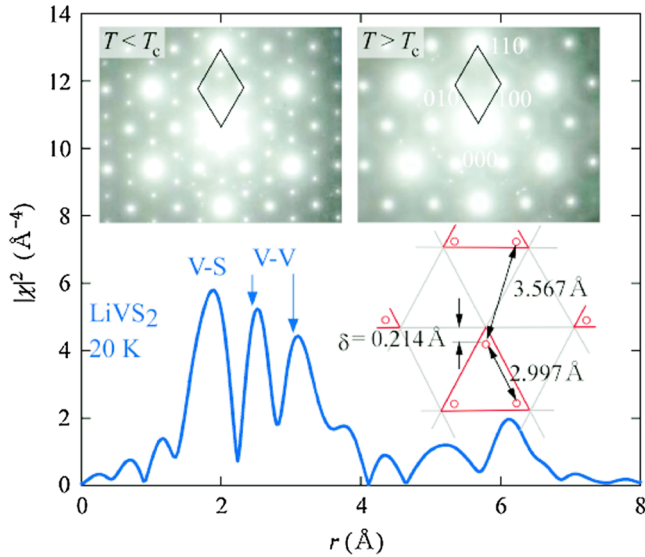


FIG. 3 (color online). Fourier transforms of the EXAFS spectra of LiVS_2 at 20 K. The lower right inset shows vanadium trimer schematically. The V-V distances and the displacement of the V from the regular triangular lattice, δ , are determined from the data taken at 200 K. The upper panels show the electron diffraction pattern along the [001] zone axis of LiVS_2 .

arrows, are ascribed to those from the first-neighbored V-V bonds, indicating the presence of two inequivalent V bonds as expected for V trimer formation. Note the large splitting of more than 10%, indicative of a local character of V trimer.

Associated with the formation of VBS state with V trimers, the volume contraction originates from the large in-plane contraction. We observed the volume contraction of $\sim 0.3\%$ as shown in Fig. 4, which is a factor of 2 smaller than that of LiVO_2 [11]. The DSC measurement shown in Fig. 4 indicates the increase of entropy $\Delta S \sim 6.4 \text{ J/mol K}$ at the VBS transition. This should give rise to a positive pressure coefficient of VBS transition temperature $dT_c/dP = \Delta V/\Delta S \sim 20 \text{ K/GPa}$ from the Clausius-Clapeyron relationship. Indeed, we observe an increase of T_c under an external pressure of a comparable magnitude (see Fig. 4), which implies that the pressure induced stabilization of VBS simply reflects the volume contraction and the low entropy in the VBS phase.

The high temperature metallic phase above $T_c \sim 305 \text{ K}$ in LiVS_2 , namely, realized at the close vicinity to VBS, is not a simple metal but a pseudogap metal. The magnetic susceptibility in this high temperature metallic phase is $\sim 5 \times 10^{-4} \text{ emu/mol}$, which yields an estimate of electronic specific heat gamma $\gamma \sim 35 \text{ mJ/mol K}^2$, assuming the Wilson ratio $R_W \sim 1$. Since R_W in correlated metals are normally 1.5–2.0, a better estimate for gamma may be $\gamma \sim 20 \text{ mJ/mol K}^2$. This is indeed consistent with the entropy change $\Delta S \sim 6.4 \text{ J/mol K}$ at the VBS transition. This ΔS for LiVS_2 is smaller than that for its insulating analogue LiVO_2 ($\Delta S \sim 14.5 \text{ J/mol K}$ [18]), indicating that

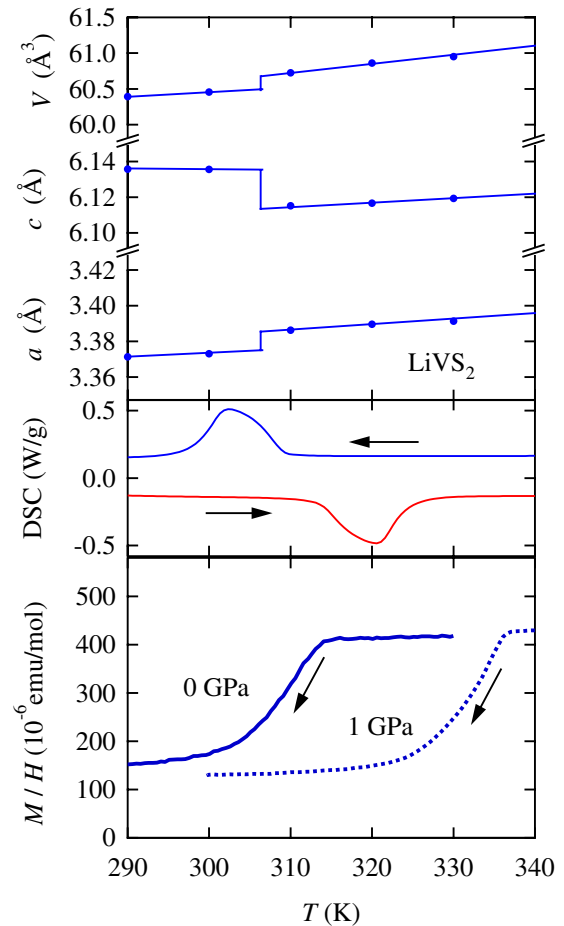


FIG. 4 (color online). The upper panel shows temperature dependence of lattice parameters a , c and the unit cell volume v . The middle panel shows DSC signals of LiVS_2 . The lower panel shows magnetic susceptibility data of LiVS_2 under hydrostatic pressure. The measurements of lattice parameters and magnetic susceptibility were performed on the cooling process, while DSC measurements were performed on both cooling and heating processes as indicated by arrows.

the high temperature metallic state of LiVS_2 has lower entropy than the high temperature phase of LiVO_2 , which may be reasonably ascribed to a Fermi degeneracy in the metallic phase. Considering that ΔS for LiVO_2 is only roughly twice of ΔS for LiVS_2 , LiVS_2 may locate close to LiVO_2 in the phase diagram, shown in Fig. 1. Assuming the observed ΔS in LiVS_2 originates from the electronic gamma $\gamma \sim 21 \text{ mJ/mol K}^2$, which is in good agreement with the estimate from the magnetic susceptibility. These estimates point to the fact that LiVS_2 at high temperatures is a paramagnetic metal with a moderate density of states at the Fermi level, comparable to those of other $3d$ transition metal chalcogenides.

In sharp contrast to the moderate magnitude, the temperature dependence of magnetic susceptibility is anomalous as a paramagnetic metal. As is clearly seen in Fig. 2, the magnetic susceptibility shows a rapid decrease on

cooling temperature, which is reminiscent of those of underdoped high- T_c cuprates with pseudogap. The same behavior of susceptibility was previously observed for a powder sample [19]. By replacing S with Se in LiVS_2 , we can suppress the VBS and increase the bandwidth further. As shown in Fig. 2, we indeed find that LiVSe_2 is a paramagnetic metal down to 2 K without any trace of anomalous decrease of susceptibility, implying that the decrease of susceptibility in LiVS_2 is associated with the proximity to the VBS state and metal to insulator transition. The ongoing systematic evolution of electronic states from O, S, to Se is clear and can be summarized by a schematic phase shown in Fig. 1. Note the increased magnitude of susceptibility in LiVSe_2 compared with LiVS_2 despite the increased bandwidth. This implies that the density of states of LiVS_2 is suppressed by some mechanism, which we take evidence of as a pseudogap. In the electron diffraction pattern of LiVS_2 in the high temperature phase (Fig. 3), we observe a diffuse scattering indicative of short-range (and dynamic) trimer formation. This leads us to speculate that the origin of pseudogap in the metallic LiVS_2 is a singlet fluctuation.

As summarized in Fig. 1, the VBS state robustly appears from the insulating side to the metallic side. VBS eventually vanishes for LiVSe_2 , perhaps due to a combined effect of the increased bandwidth and the lattice expansion. VBS formation in LiVO_2 had been discussed in terms of novel interplay of spin and orbital degrees of freedom in geometrically frustrated magnet [20]. The presence of VBS over the metal to insulator crossover region suggests that, in contrast to the conventional picture, electron transfer (itinerancy) might play a certain role in realizing the VBS, as in the orbitally driven Peierls transition in CuIr_2S_4 and MgTi_2O_4 [21].

Very recently, Itou *et al.* demonstrated the absence of pseudogap in the superconducting $\text{EMe}_3\text{P}[\text{Pd}(\text{dmit})_2]_2$ by NMR measurement [22], indicating that the pseudogap metallic state is unique to the present LiVX_2 system. It may be interesting to further suppress VBS from LiVS_2 to $T = 0$ with substitution of S with Se and to explore the exotic metal formed near the possible VBS critical point. In the $\text{LiVS}_{2-x}\text{Se}_x$ solid solution, we indeed observed a systematic decrease of the magnetic susceptibility anomaly representing the VBS transition upon Se substitution and a disappearance around $x = 0.3$, shown in the right inset of Fig. 1. We found, however, that all of the Se substituted samples show a weakly insulating behavior, perhaps due to the disorder effect inherent to the Se substitution, and that the exotic metal phase including superconductivity could not have been explored.

In conclusion, we have identified a crossover from the $S = 1$ Mott insulator to a paramagnetic metal in a series of

triangular lattice vanadates, LiVX_2 with $X = \text{O}, \text{S}$, and Se . LiVS_2 is located at the crossover region, and a paramagnetic metal to the valence-bond solid (VBS) insulator transition was observed as a function of temperature. We argue that the high temperature metallic phase in LiVS_2 is a pseudogap metal with possible spin-singlet correlation due to the close proximity to the VBS state, which provides a new playground for the novel interplay of strong electron correlation and the geometrical frustration.

The authors are grateful to D. I. Khomskii, Y. Motome, and T. Itou for valuable discussions. This work was partly supported by a Grant in Aid for Scientific Research (No. 16076204) and the ‘‘Nanotechnology Support Project’’ of the Ministry of Education, Culture, Sports, Science and Technology of Japan.

*Present address: Department of Physics, University of Virginia, 382 McCormick Road, Charlottesville, VA 22904, USA.

nk2u@cms.mail.virginia.edu

†Present address: Department of Physics, Okayama University, 3-1-1 Tsushima-naka, Okayama 700-8530, Japan.

- [1] J. B. Goodenough *et al.*, Phys. Rev. B **43**, 10 170 (1991).
- [2] M. Onoda *et al.*, J. Phys. Soc. Jpn. **60**, 2550 (1991).
- [3] M. Onoda and T. Inabe, J. Phys. Soc. Jpn. **62**, 2216 (1993).
- [4] K. Imai *et al.*, J. Solid State Chem. **114**, 184 (1995).
- [5] W. Tian *et al.*, Mater. Res. Bull. **39**, 1319 (2004).
- [6] Y. Horibe *et al.*, Phys. Rev. Lett. **96**, 086406 (2006).
- [7] M. Schmidt *et al.*, Phys. Rev. Lett. **92**, 056402 (2004).
- [8] P. G. Radaelli *et al.*, Nature (London) **416**, 155 (2002).
- [9] M. Tamura *et al.*, J. Phys. Soc. Jpn. **75**, 093701 (2006).
- [10] Y. Shimizu *et al.*, Phys. Rev. Lett. **99**, 256403 (2007).
- [11] S. Kobayashi *et al.*, Mater. Res. Bull. **4**, 95 (1969).
- [12] G. Oomi *et al.*, J. Magn. Magn. Mater. **140–144**, 157 (1995).
- [13] B. van Laar and D. J. W. Ijdo, J. Solid State Chem. **3**, 590 (1971).
- [14] D. W. Murphy *et al.*, Inorg. Chem. **16**, 3027 (1977).
- [15] The stacking along the c axis is the $1T$ type (space group: $P\bar{3}m1$) for LiVS_2 and LiVSe_2 , while the stacking along the c axis is the $3R$ type (space group: $R\bar{3}m$) for LiVO_2 in the Ramsdell notation.
- [16] D. W. Murphy *et al.*, Inorg. Chem. **15**, 17 (1976).
- [17] T. Tanaka, Y. Kawasaki, S. Endou, S. Kimura, Y. Ideta, Y. Kishimoto, T. Ohno, N. Katayama, M. Nohara, and H. Takagi, J. Phys. Soc. Jpn. **78**, 054709 (2009).
- [18] S. Niitaka (private communication).
- [19] F. J. DiSalvo, J. V. Waszczak, and M. Eibschutz, Phys. Rev. B **24**, 5143 (1981).
- [20] H. F. Pen *et al.*, Phys. Rev. Lett. **78**, 1323 (1997).
- [21] D. I. Khomskii and T. Mizokawa, Phys. Rev. Lett. **94**, 156402 (2005).
- [22] T. Itou *et al.*, Phys. Rev. B **79**, 174517 (2009).